International Conference on Applied Energy 2021
Nov. 29 - Dec. 2, 2021, in Bangkok, Thailand
Paper ID: 0143

Phase-change -based Thermal Protection for Pulsed Electrical Machines

Xia Chen[1], Mingliang Zhong[2], Yufeng Mao[2], Jixiang Wang [1,2,3,4*]

1 Key Laboratory of Energy Thermal Conversion and Control of Ministry of Education, School of Energy and Environment, Southeast University, Nanjing, 210096, P. R. China (Corresponding Author)

2 Institute of Optics and Electronics, Chinese Academy of Sciences, Chengdu, 610209, PR China

3 Department of Mechanical and Aerospace Engineering, The Hong Kong University of Science and Technology, Hong Kong, PR China

4 College of Electrical, Energy and Power Engineering, Yangzhou University, Yangzhou, 225009, PR China

ABSTRACT

The concept of "more and all electric plane" has been running high in the last two decades, which will boost the extensive utilization of air-borne electrical actuators such as permanent magnet synchronous machines (PMSMs). Thus, considerable waste heat will be generated inevitably during their operation due to the incomplete energy conversion, which would be a great challenge for the conventional onboard thermal control system. It would lead to a sharp temperature rise in thermal-sensitive components of the onboard devices if the huge generated heat cannot be removed efficiently. This overheating will cause operational failures which are intolerable in aerospace applications. For the purpose of improving the current thermal protection measures and gain a higher compatibility of the current PMSM system aboard, a phase change material based (PCM-based) thermal protection strategy using commercial wax is proposed in this paper. Comparative investigation was organized to show that the temperature did drop down, demonstrating the advantages of deploying the proposed PCM-based cooling scheme. Further data processing using partial derivative to attain a relative optimal operating condition. Such method can be promoted to wider applications using PCM as a cooling medium as dimensionless study was conducted in this paper.

Keywords: phase change material, thermal energy storage, heat transfer, thermal control, aerospace engineering

NONMENCLATURE

Abbrevations	
PCM	Phase change material
PMSM	Permanent magnet synchronous machine
EQ	Equivalent
DHP	Dimensionless heat power
TSD	Temperature spike difference
CDHP	Critical dimensionless heat power
DTSD	Dimensionless temperature spike difference
Symbols	
ω	DHP
γ	Period (s)
ε	Duty cycle
P	heat power (W)
τ	DTSD
θ	Dimensionless thermal conductivity
ΔT_{peak}	TSD (°C)
Nu_i	The Nusselt number for the surface i
$T_{ave,\mathrm{II},EQ\mathrm{II}}$	Average temperature of Location II of EQ-Machine II

1. INTRODUCTION

Permanent magnet synchronous machines (PMSMs), which are one of the most significant components in energy conversion systems, have been widely used in traction applications and industrial processes such like packaging, portaging and fixing[1] due to their light mass, small volume, simple structure and high efficiency. In addition, as the concept of "more and all electrical aircraft" has been running high in recent years, it is obvious that a number of the on-board PMSMs which function as substitutions of the traditional air-oriented hydraulic, pneumatic, and mechanic systems are anticipated to be deployed aboard extensively in the coming years. Taking the fact that the reliability is the most critical factor for aerospace applications into

Selection and peer-review under responsibility of the scientific committee of the 13th Int. Conf. on Applied Energy (ICAE2021).

account, how to improve the reliability of the thermal-sensible components such as permanent magnets, stator winding insulation, and bearings inside the on-board PMSMs is the main task for the aerospace scientists and engineers.

Initial solid-phase volume(m3)	1.38×10-4
Specific heat capacity (kJ·kg-1·K-1)	2.6
Density (Solid-phase) (kg/m3)	910
Thermal conductivity (W/m·K)	0.52
Enhanced thermal conductivity (W·m-1·K-1)	27.78

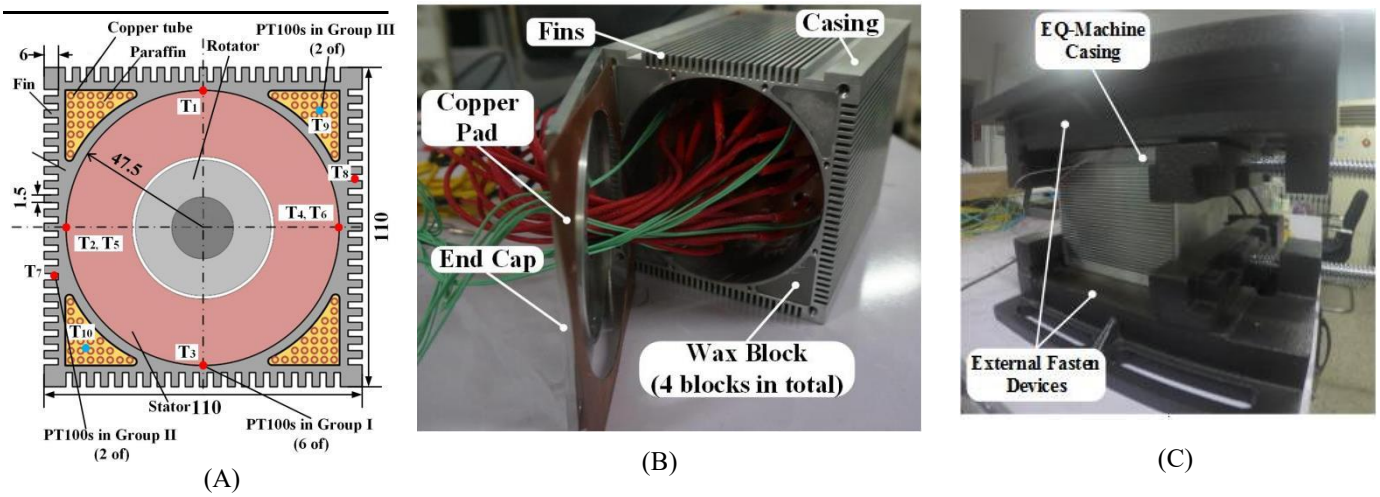

Fig. 1. EQ-Machine integrated with PCM-based thermal protection strategy and experimental set-up. (A) Schematic view of the EQ-Machine. (B) Photographic view of the EQ-Machine. (C) Physical EQ-machine with the fasten device.

Table 2 Description of operating conditions

Case	Period (s)	Duty cycle	Heat Power (W)	DHP
1	1500	13.30%	313, 350, 388, 429, 471, 510, and 550	2.47, 2.76, 3.06, 3.38, 3.71, 4.02, and 4.33
2	1500	20%	168, 216, 246, 279, 313, 365 and 400	1.99, 2.56, 2.92, 3.31, 3.71, 4.33, and 4.74
3	1500	26.70%	140, 168, 195, 216, 246, 313 and 365	2.21, 2.66, 3.08, 3.42,3.89, 4.95 and 5.77

In this paper, an air-borne PMSM is our target electrical actuator which is prone to an intermittent operating model. Hence the corresponding heat generation pattern abides by an alternate heating and cooling events. The temperature mismatch existing between intermittent operations can be narrowed by employing thermal energy stroage system[2]. The primary goal of the present study is to establish practical experimental PMSMs with and without commercial-available waxes, upon which thermal tests were conducted. Comparative study was organized to investigate the superiorities of employing wax quantitatively. Based on the first-hand data, dimensionless study was conducted to optimize the phase-change-material-based cooling system using a novel data processing method.

2. EXPERIMENTAL APPARATUS AND RELATIONS

2.1 Equivalent (EQ)-Machine Integrated with PCM-based Thermal Protection Measure

Table 1 Parameters of the selected wax.

Properties	value

For the purpose of security, the two identical EQ-Machines with and without PCM-based cooling scheme were adopted in the present experimental study. For the conciseness of the following description, we define the EQ-Machine utilizing PCM-based cooling scheme as EQ-Machine I and the EQ-Machine without PCM-based thermal protection measure EQ-Machine II. The EQ-Machine I is displayed in Fig. 1. In order to achieve a higher compatibility of the current PMSM system, four holes were drilled throughout the PMSM casing prepared for the wax injection.

The related properties of the selected wax employed in the present study are listed in Table 1. The melting point of the selected wax is measured to be 78.81 °C and latent heat 201.6 kJ/kg. Therefore, the total latent heat of the wax is 25316.9 J. In Addition, For the purpose of resolving wax's extremely low heat conductivity, several tiny cooper tubes were embedded in the blocks of the utilized wax which is displayed in Fig. 1 (A). The volumetric ratio of the cooper tube is calculated to be approximately 0.07. Therefore, the integrated thermal conductivity of the adopted copper-wax composite is listed in Table 1 as well.

As shown in Fig. 1 (A), three groups of PT100s (Group I, II, and III) were arranged in each EQ-Machine to detect the temperatures of three critical locations (Location I, II and III). Location I represents the interface between the internal surface of the casing and the external one of the winding, Location II outer surface of the casing and Location III wax blocks. There are six PT100s (T_1-T_6) in Group I, two PT100s (T_7-T_8) in Group II, and two PT100s (T_9-T_{10}) in Group III. Since the EQ-Machine II is not equipped with the PCM-based thermal protection strategy, PT100s of Group III were not arranged.

2.2 *Description of experimental apparatus*

Fig. 1 (C) demonstrates the schematic of the test setup. An external fasten device was added for preventing the leakage of the wax. To ensure an identical thermal environment, EQ-Machine I and II were fixed on the thermal-insulating board. Both windings of EQ-Machines are connected to a DC power supply and a signal generator to control the heat power of the EQ-Machines in a desired duty cycle according to practical pattern of the real pulsed PMSM's thermal behavior.

As the practical PMSM is subject to an "on/off" cycle, the course of the thermal behavior abides by a periodic heating pattern. Thus the operating conditions in the thermal tests are listed in Table 2. To prepare for theconduction of the dimensionless study, a dimensionless parameter called dimensionless heat power (DHP) ω , which is calculated by $\omega = \gamma\varepsilon P / V_w \rho_w \eta_w$,(V_w , ρ_w and η_w are the solid-phase volume, density and latent heat of the wax.) is also listed in Table 2. Each condition would be conducted upon EQ-Machine I and II respectively for comparative study. The ambient temperature was sustained to be 21±1 °C during all the thermal tests.

The maximum uncertainty of the PT100 was calculated to be ± 0.5 °C. And the heat power's uncertainty was estimated to be ±1.8%.

3. RESULTS

3.1Transient temperature analysis

Transient temperature profiles of different operating cases are analyzed. As shown in Fiq. 2 (A), In each cycle, the wax's temperature climbs up firstly when the PMSM is heated, and then the temperature begins to drop when the heating process ends. However, the slope of the descending temperature curve is relatively small, indicating that a specific mass of wax is still in its solid state when the cooling down process starts. It can be concluded that both operating conditions fail to maximize the benefits of the wax. By contrast, The wax's temperature curve in Figure 5 (D) manifests a clear difference compared with that in Figure 5 (A) and (B) where the cooling down course shows a continuous huge slope. It is indicated that the wax is in its liquid phase when the heating process in the next cycle starts in which the advantage of the involvement of the wax is swallowed as the relatively large amount of heat power has overwhelmed the latent heat of the wax. In such conditions, the wax remains to be liquid-phase even in the cooling process, resulting in exhaustion in the utilizing of the latent heat and a block in the heat-dissipating path due to the low thermal conductivity of the wax. Therefore, the temperature spike difference (TSD), calculated by $\Delta T_{peak} = T_{peak,I,II} - T_{peak,I,I}$, will be waived under these conditions. A coherence in the DHP can be spotted when the data is plotted as the TSD in the x axis and the DHP in the y axis, which is shown in Figure 3. It can be observed that optimal DHPs which can also be named by critical DHPs (CDHPs) for Cases 1, 2, and 3 are 3.52, 3.67, and 3.70. Therefore, the average CDHP is 3.63.

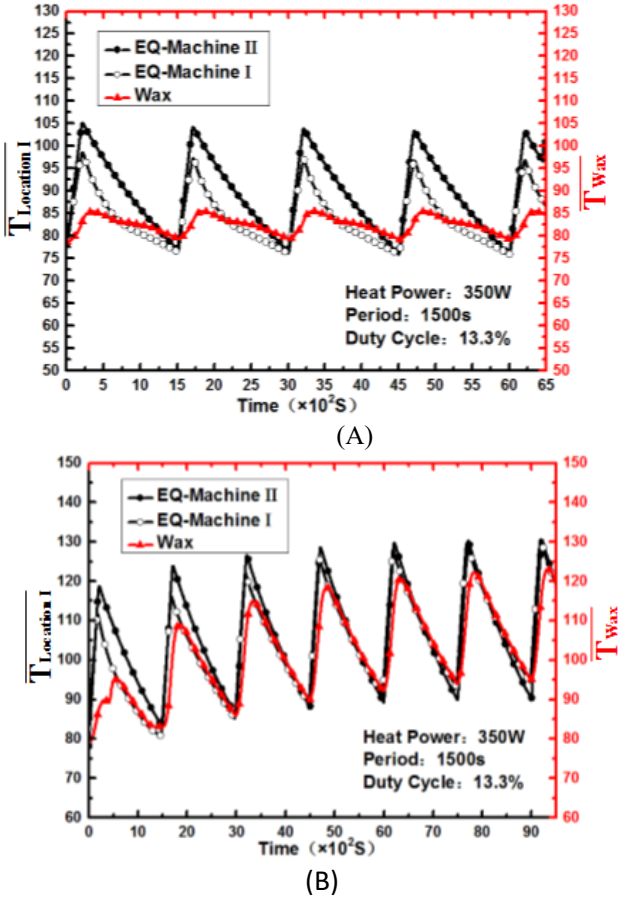

Fig. 2. Typical transient performances for EQ-Machine I and II in Case 1. (A) 350W (DHP is 2.76). (B) 550W (DHP is 4.33).

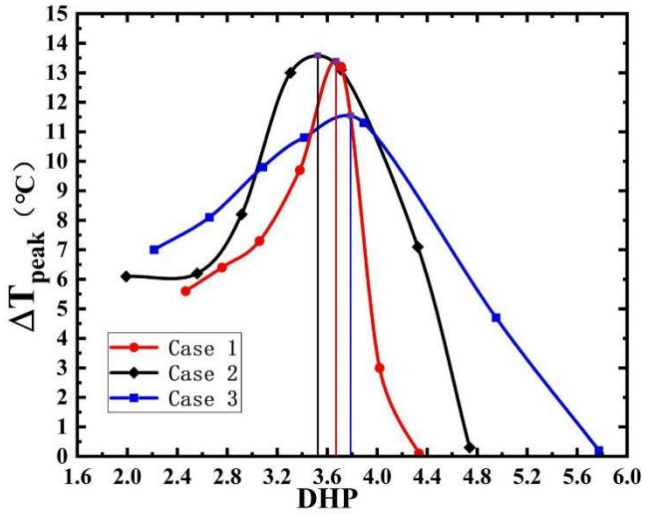

Fig. 3. TSD as a function of DHP in three cases.

3.2Dimensionless study

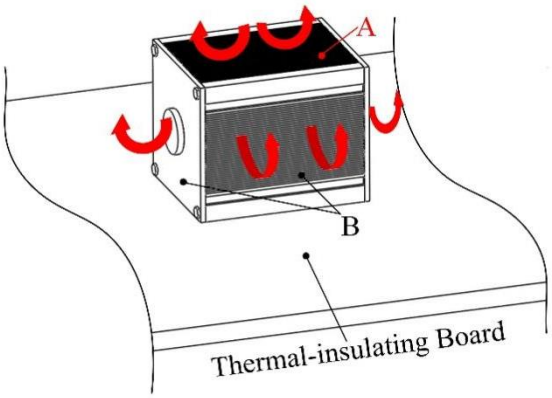

Fig. 4. Natural convection of the the EQ-Machine casing

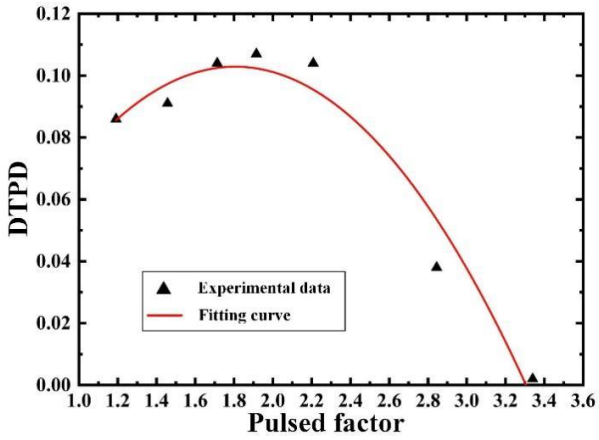

Fig. 5. DTPD as a function of the pulsed factor.

It is acknowledged that cooling performance enhancement which should be represented by TSD in the present study is governed by several conditions including the external natural convection heat-transfer circumstance, thermal conductivity of the wax-copper composite, and the DHP. The Natural convection, which can be determined by Nusselt number Nu that can be calculated by the Grashof number which is calculated by $Gr = g\alpha(T_{Location,\mathrm{II}} - T_a)l^3/\upsilon^2$. The generated heat is primarily rejected in the form of natural convection by five surfaces (one surface A and four surface B) of the EQ-Machine casing as shown in Figure 4. the Nu_A is calculated by $Nu_A = 0.54(Gr_A Pr_A)^{0.25}$, the Nu_B by $Nu_B = 0.59(Gr_B Pr_B)^{0.25}$ and the overall Nu by Equation $Nu = 0.25Nu_A + 0.75Nu_B$. The dimensionless thermal conductivity θ is gained by $\theta = \lambda_w / \xi\lambda_{cu}$. Dimensionless TSD (DTSD) can be deduced by $\tau = \Delta T_{peak} / T_{ave,\mathrm{II},EQ\mathrm{II}}$. Hence the heat transfer correlated equation can be adopted by $\tau = f(Nu, \omega, \theta)$. The solution of $\partial f(Nu, \omega, \theta)/\partial Nu\,\partial\theta = 0$. is the CDHP ω_c . We found the $\tau = f(Nu, \omega, \theta)$ can be expressed by $\tau = -0.04632 + 0.16524\kappa - 0.04575\kappa^2$ where κ is defined as the pulsed factor that can be calculated by $\kappa = \omega \times \theta \times Nu$ using the experimental data. Therefore, the predicted optimal pulsed factor is 1.81 where it can attain the highest DTSD. In this condition, the CDHP is calculated to be 3.38 against the test deduced value of 3.63 from the experimental data with a relative error of only 6.8%.

4. CONCLUSIONS

In order to gain an improvement in the current onboard thermal protection system of the pulsed PMSM in more-electric planes, a PCM-based thermal protection strategy is adopted in this paper.

The biggest innovation of this paper is the quantitative dimensionless study where the pulsed factor considering most influencing factors is proposed. The derived optimal pulsed factor may have industrial value in the related area of PCM-based thermal protection system not confined to the given conditions described in this paper. Further verification by using different amounts of PCM or different species of the PCM will be conducted in our future investigation.

REFERENCE

[1] Pettersson M, Ölvander J. Drive train optimization for industrial robots. IEEE Trans. Robotics. 2009;25(6):1419-1424.

[2] Beyhan B, Paksoy H, Dasgan Y. Root zone temperature control with thermal energy storage in phase change materials for soilless greenhouse applications. Energy Convers Manage. 2013;74(5): 446-453.